Top Catal (2013) 56:969–980
DOI 10.1007/s11244-013-0061-y

Low Temperature Catalytic Decomposition of Hydrogen Sulfide into Hydrogen and Diatomic Gaseous Sulfur

A. N. Startsev · O. V. Kruglyakova · Yu. A. Chesalov · S. Ph. Ruzankin · E. A. Kravtsov · T. V. Larina · E. A. Paukshtis

Published online: 24 May 2013

Abstract A new catalytic reaction of hydrogen sulfide decomposition is discovered, the reaction occurs on metal catalysts in gas phase according to equation

$$2H_2S \leftrightarrow 2H_2 + S_2^{(gas)}$$

to produce hydrogen and gaseous diatomic sulfur, conversion of hydrogen sulfide at room temperature is close to 15 %. The thermodynamic driving force of the reaction is the formation of the chemical sulfur–sulfur bond between two hydrogen sulfide molecules adsorbed on two adjacent metal atoms in the key surface intermediate and elimination of hydrogen into gas phase. "Fingerprints" of diatomic sulfur adsorbed on the solid surfaces and dissolved in different solvents are studied. In closed vessels in adsorbed or dissolved states, this molecule is stable for a long period of time (weeks). A possible electronic structure of diatomic gaseous sulfur in the singlet state is considered. According to DFT/CASSCF calculations, energy of the singlet state of S_2 molecule is over the triplet ground state energy for 10.4/14.4 kcal/mol. Some properties of gaseous diatomic sulfur are also investigated. Catalytic solid systems, both bulk and supported on porous carriers, are developed. When hydrogen sulfide is passing through the solid catalyst immersed in liquid solvent which is capable of dissolving sulfur generated, conversion of hydrogen sulfide at room temperature achieves 100 %, producing hydrogen in gas phase. This gives grounds to consider hydrogen sulfide as inexhaustible potential source of hydrogen—a very valuable chemical reagent and environmentally friendly energy product.

Keywords Hydrogen sulfide decomposition · Hydrogen production · Diatomic gaseous sulfur · Reaction thermodynamics · Sulfur electronic structure

1 Introduction

Hydrogen is one of the most claiming chemical substances widely used in many large-scale processes of industry, and demand for its consumption is growing with advanced rate. The point is that hydrogen is forecasted to become a major source of energy in the future [1–4]. Currently, steam reforming of hydrocarbons is the largest and generally the most economical way to produce hydrogen; however, the search for new chemical technologies of hydrogen production is continuously accomplishing, especially from renewable resources [5]. One of such practically inexhaustible sources of hydrogen could be hydrogen sulfide, H_2S. In contrast to water, hydrogen is only loosely bound in the hydrogen sulfide molecule (standard enthalpy of formation $\Delta_f H_{298}^\circ = -4.82$ kcal/mol for H_2S and $\Delta_f H_{298}^\circ = -57.80$ kcal/mol for H_2O). In comparison, $\Delta_f H_{298}^\circ = -17.89$ kcal/mol for methane. That means lower energy inputs for H_2S dissociation into constituent elements.

Large amounts of hydrogen sulfide are produced worldwide, both in nature and industry, mostly from natural gas production and oil refining. Hydrogen sulfide is emitted by some plant species as a byproduct of sulfite metabolism. Estimates of the terrestrial emission rate of H_2S range from 58 to 110 million tons of sulfur/year and from oceans—from 30 to 170 million tons of sulfur/year. The Black Sea is unique basin because 90 % of sea water is

A. N. Startsev (✉) · O. V. Kruglyakova · Yu. A. Chesalov · S. Ph. Ruzankin · E. A. Kravtsov · T. V. Larina · E. A. Paukshtis
Boreskov Institute of Catalysis, Novosibirsk, Russia
e-mail: Startsev@catalysis.ru

anaerobic and contains hydrogen sulfide produced by sulfur reducing bacteria. The total amount of H_2S in Black Sea is estimated to be 4.6 billion tons, which may potentially be recovered into 270 million tons of hydrogen [6].

Hydrogen sulfide occurs as a by-product in the treatment of almost all natural raw materials used for energy production, i.e. natural gas, crude oils and coals. The hydroprocessing of petroleum, coal and minerals yields above 60 million tons per year of toxic H_2S and thus, in addition to H_2S presented in natural gas, the utilization of H_2S is the major objective of gas processing technology. The resulting toxic H_2S is often removed via Claus process and caustic or alkanolamine absorption. These routes permit only the recovery of elemental sulfur, while H_2 is simply jettisoned as water.

At the same time, hydrogen sulfide is one of the most toxic substances with characteristic odor of rotten eggs; odor threshold in air is 0.5 ppb [7]. Therefore, all waste gases of any manufactories must be carefully purified from hydrogen sulfide.

The direct thermal decomposition of hydrogen sulfide into hydrogen and sulfur

$$H_2S \leftrightarrow H_2 + 1/2\,S_2 \quad (1)$$

is a highly endothermic process: $\Delta_r H_{298}^\circ = 20.25$ kcal/mol, $\Delta_r S_{298}^\circ = 9.25$ cal/mol K, $\Delta_r G_{298}^\circ = 17.5$ kcal/mol [8]. Detailed investigations of equilibrium conversion of hydrogen sulfide into hydrogen and gaseous products of molecular sulfur S_i ($i = 1, \ldots, 8$) have shown that at temperature below 800 K the total conversion of H_2S does not exceed 1.5–2 % taking into account the concentrations of all components in the equilibrium mixture $H_2S/H_2/S_i$ [9]. H_2S conversion is increasing at temperature raising and total pressure decreasing. To shift the equilibrium of reaction (1) to the right, well-known techniques of reaction product separation and different energy sources are used [10, 11]; however, none of them found commercial application because of high cost of hydrogen produced [12].

It is generally known that a catalyst does not shift reaction equilibrium, but it can initiate and direct the chemical reaction in such a way that the thermodynamically unfavorable process could be realized. Recently [13, 14], we have found the reaction of hydrogen sulfide decomposition into constituent elements can occur over sulfide catalysts at room temperature. The thermodynamic driving force of this process is the surface stoichiometric reaction between two H_2S molecules adsorbed on two adjacent metal atoms, which results in the formation of sulfur–sulfur bond in the surface intermediate $(H_2S_2)_{(ads)}$ and the removal of hydrogen molecule into gas phase:

$$2(H_2S)_{ads} \rightarrow (H_2S_2)_{ads} + H_2 \uparrow \quad (2)$$

this exothermic reaction ($\Delta_r H_{298} = -16.2$ kcal/mol [14]) occurs spontaneously at room temperature on the surface of sulfide catalysts ($\Delta_r G_{298} = -10.3$ kcal/mol [14]), and division of reaction products results in the reaction (2) to be irreversible. The limiting stage of catalytic reaction is decomposition of the key surface intermediate $(H_2S_2)_{ads}$ resulting in removal of the second hydrogen molecule into gas phase and recombination of surface diatomic sulfur into cyclooctasulfur S_8 [13, 14]. It should be noted that the reaction of disulfane formation

$$2H_2S \neq H_2S_2 + H_2 \quad (3)$$

is thermodynamically prohibited in gas phase [8], but occurs on the catalyst surface [15, 16]. Hence, the catalyst accomplishes very executive and specific function: after H_2S adsorption it creates conditions to form a new chemical sulfur–sulfur bond between molecules adsorbed resulting in initiation of a new catalytic route of hydrogen sulfide decomposition. For the first time, the formation of disulfane as an intermediate on the surface of metallic catalysts was observed by Raymont [17] with high temperature ultraviolet spectroscopy and nuclear magnetic resonance technique.

Despite the reaction of hydrogen sulfide decomposition occurs on sulfide catalysts in a periodical regime with low efficiency, the thermodynamic possibility to realize it at room temperature served as the basis for searching such catalysts that could provide acceleration of the reaction limiting step—decomposition of the key surface intermediate into the final products. The essential requirement to the catalysts is that the active component must be stable in H_2S atmosphere and does not form low-active metal sulfides. One of the suitable candidates is platinum.

This paper deals with studying the main regularities of low temperature decomposition of hydrogen sulfide on metallic catalysts, both bulk and supported. Three possible regimes of the reaction are investigated—flow gas phase, autoclave and triple phase, when solid catalyst is immersed into a layer of solvent.

2 Experimental and Theoretical

Hydrogen sulfide was produced in the pilot-chemical workshop of the Boreskov Institute of Catalysis by passing of hydrogen through a mixture (commercial sulfur + sulfide catalysts) heated to 400 °C. Oxygen content in H_2S produced did not exceed 0.05 % vol.

To prepare supported catalysts, silica, alumina and carbon material Sibunit with $S_{BET} = 200$–220 m^2/g and pore volume 0.6–0.8 cm^3/g were used as a carrier. Pt was supported by impregnation of a carrier with aqueous solution of H_2PtCl_6, followed by drying under IR lamp and calcinations in air at 400 °C. In the similar manner, the metallic catalysts supported on silica (BIC-24-8), alumina

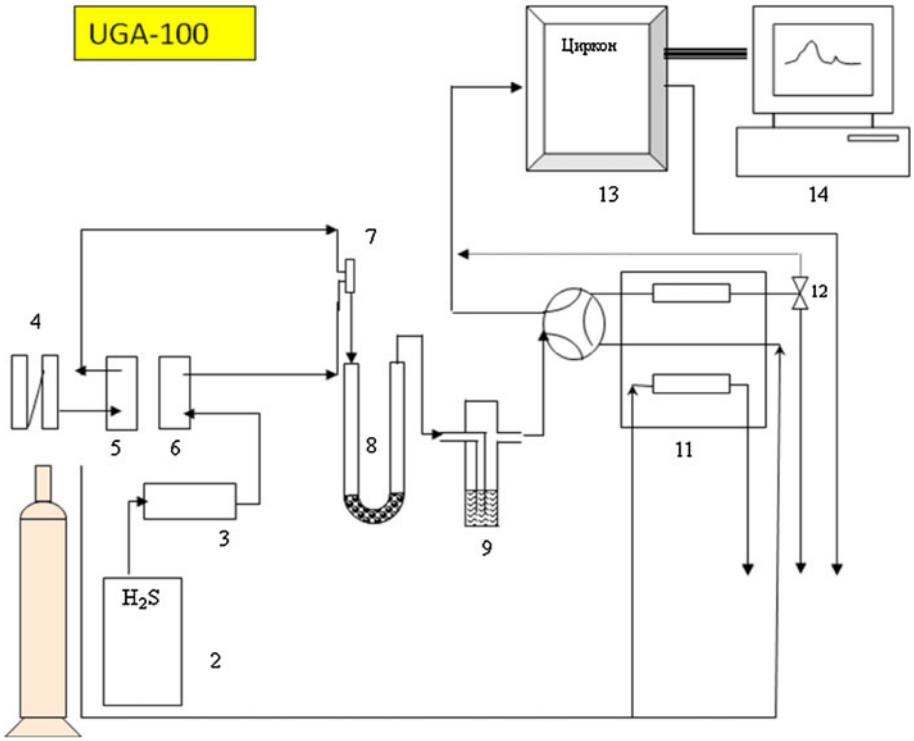

Fig. 1 Experimental setup for low temperature decomposition of hydrogen sulfide. *1* Ar cylinder; *2* H_2S cylinder; *3* cleaning unit of H_2S from O_2; *4* units with reduced Ni–Cr catalyst and zeolite NaX for Ar cleaning from oxygen and water; *5,6* flow mass controller for Ar and H_2S, respectively; *7* flow gas mixture; *8* glass reactor; *9* absorber(s) with aqueous zinc acetate solution; *10* flow gas sampler; *11* gas chromatograph Zwet; *12* shut-off cock; *13* hydrogen analyzer Zircon; *14* computer. UGA-100 is a quadruple mass spectrometer—universal gas analyzer, Stanford Research Systems

(BIC-24-9) and Sibunit (BIC-24-10) were prepared. The catalysts contain non-noble metals and are prepared from aqueous solutions of cheap and non-toxic metal salts. Before testing in catalytic reaction, all catalysts were reduced in hydrogen flow at 400 °C. The bulk catalyst BIC-24-7 is chips made from a pig of non-corrosive metal.

The gas-flow experimental rig to study hydrogen sulfide decomposition is shown in Fig. 1. The flow of argon is mixing with hydrogen sulfide flow in a definite proportion and passing through the catalyst. At the reactor outlet, two absorbers (the second one for control) with aqueous zinc acetate solution serve as a trap for unreacted hydrogen sulfide collection and are used for quantitative analysis of hydrogen sulfide conversion. After H_2S separation, composition of reaction mixture is analyzed with a gas chromatograph Zwet-500 and hydrogen detector Zircon. The catalyst activities are compared as the amount of hydrogen sulfide converted into the reaction products during the time-on-stream period and related to the amount of metals in catalysts. To study the triple-phase regime, solid catalyst is placed in a glass mixer under a layer of solvent equipped with a magnetic stirrer. In autoclave regime, a high pressure cylinder of 300 cm^3 was used. On the bottom of autoclave, 40–60 g of a freshly calcined carrier (alumina, silica, Sibunit) was loaded and from above through a partition made of fiberglass, 5 g of a catalyst was placed. After evacuation till 10^{-2} torr, 4–6 g of liquid H_2S was introduced by autoclave cooling.

Quantitative analysis of H_2S was conducted according to [18] by its extraction from gas flow with 5–40 wt% aqueous solution of zinc acetate. ZnS formed is decomposed in acid media, while hydrogen sulfide evolved is determined with iodine titration.

Raman spectra were recorded with a spectrometer FT-Raman RFS 100/S BRUKER (Germany) in the region of 100–3,600 cm^{-1}. The excitation source is the line at 1,064 nm of Nd-YAG laser with power of 450 mW.

Infrared spectra were recorded with a spectrometer Shimadzu 8300 equipped with a diffuse reflection device DRS-8000 in the region of 400–6,000 cm^{-1} with resolution of 4 cm^{-1} and accumulation of 200. Spectra of adsorbed molecules were detected by subtraction of background from the analyzed spectra.

Chemical composition of solid and liquid substances was monitored with a fluorescent X-ray analyzer ARL-Advant'x with Rh anode of X-ray tube.

All calculations were made using the Gaussian 09 program package [19]. The electron structure calculations were made in the DFT framework using hybrid exchange–correlation functional B3LYP [20–23], and ground state and excited states were calculated also by CASSCF method involving the active space (6 electrons, 6 molecular orbitals). The basis set was 6-311++G(d,p) [24, 25]. The orbitals were drawn by means of ChemCraft program [26]. The DFT/B3LYP calculations of S_2 molecule were carried out for three electronic states: the triplet (ground state), the closed shell singlet and the singlet with a spin broken symmetry (BS-singlet). The ground state (triplet) and 1st

excited singlet were calculated also using CASSCF (6e,6MO) method.

3 Results

On passing H_2S through metallic catalysts at room temperature, two gaseous reaction products are detected with a gas chromatograph (Fig. 2) (remind: non-reacted H_2S is collected in absorber with zinc acetate). Evolution of both products is synchronous; after short "breakdown" period attendant upon increasing H_2S concentration on the catalyst surface, in 40 min of time-on-stream the gas-phase concentration of both products is increasing until constant level. The first product is true hydrogen (proved by introduction of pure hydrogen in a gas flow). The nature of the second product was identified in the following experiments.

An absorber with aqueous monoethanolamine (MEA) solution was placed after the first absorber with zinc acetate, and reaction of H_2S decomposition was carried out in a typical manner (Table 1). In gas phase, only hydrogen was detected with a gas chromatograph, the second product was absent. The material balance has shown that the amount of sulfur trapped in a MEA solution is exactly the same as H_2S decomposed. In another experiment, instead of MEA, an absorber with pyridine was placed and reaction was carried out once again. Only hydrogen was detected in gas phase as well. In the Raman spectra of pyridine solution, a set of bands characteristic of solid sulfur dissolved in pyridine was observed (Fig. 3). As follows from both experiments, the gaseous sulfur is the second reaction product of H_2S decomposition. According to mass-spectra, this gaseous sulfur has an atomic mass of 64 m/z (Fig. 4), hence to the second gaseous product of H_2S decomposition the formula S_2 must be attributed.

To exclude another possible sulfur containing products, the following arguments should be taken into account. Oxygen is "the worst enemy" of the reaction of H_2S decomposition, therefore all gases and solvents were carefully purified from oxygen. Even traces of oxygen provoke the reaction of H_2S oxidation to form solid sulfur and water (not hydrogen!). SO_2 has an atomic mass of 64 m/z as well, but this molecule must be excluded because it cannot form in absence of oxygen, and even though it happened, this molecule cannot pass through aqueous solution of zinc acetate. Moreover, in Raman spectra no stretching modes of S–O and S–H bonds were found (Fig. 3).

Table 2 summarizes activity of the 0.5 % Pt/SiO_2 catalyst in a set of consecutive experiments on H_2S decomposition. After 60 min of each experiment, H_2S feeding was stopped, the setup was blown down with Ar to collect non-reacted H_2S into absorber with zinc acetate, and the next experiment was carried out. The average H_2S

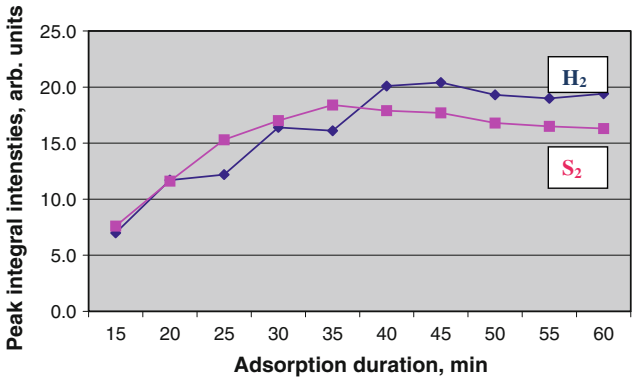

Fig. 2 The typical chromatograph diagram of evolution of gaseous products during H_2S decomposition over metallic catalysts at room temperature

Table 1 Hydrogen sulfide decomposition on the bulk catalyst BIC-24-7 at room temperature

Argon feeding (ml/min)	10
Hydrogen sulfide feeding (mmol/min)	0.0803
Amount of H_2S supplied (mmol)	4.82
Amount of H_2S non-reacted (mmol)	4.69
H_2S conversion (%)	2.7
Amount of H_2S converted (mmol)	0.13
Volume of 5 % MEA solution (ml)	100
Concentration of sulfur in MEA solution (mass %)[a]	0.0042
Amount of sulfur in MEA solution (mg-at)	0.13

Mass of catalyst is 2.7 g

[a] X-ray fluorescent analysis

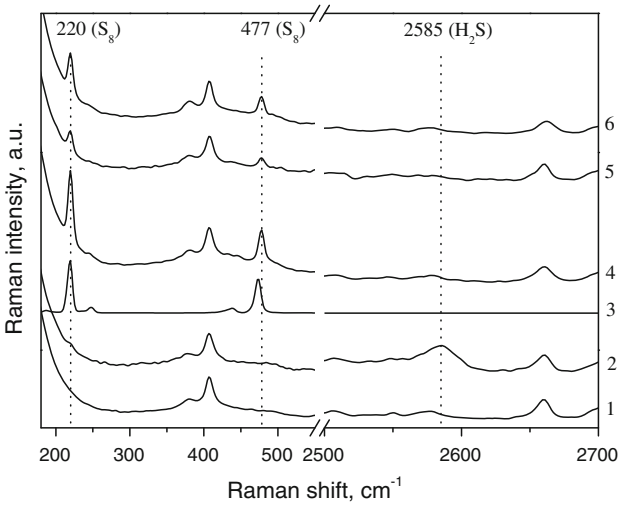

Fig. 3 Raman spectra of sulfur solutions in pyridine. *1* Pyridine; *2* H_2S solution in pyridine; *3* solid sulfur S_8; *4* solid sulfur solution in pyridine; *5,6* pyridine solution of gaseous S_2

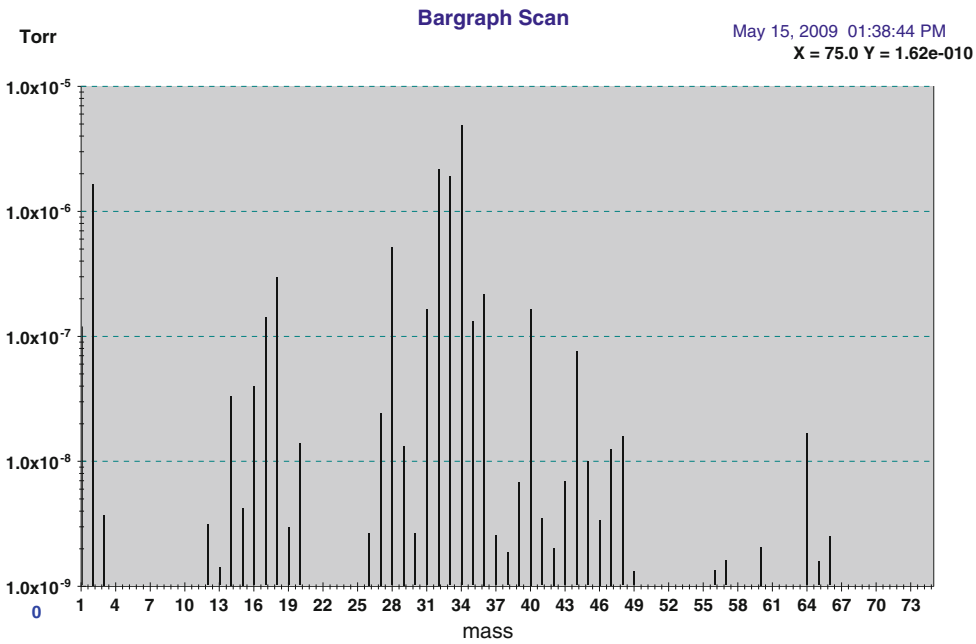

Fig. 4 Mass-spectrum of the equilibrium composition of the reaction products of H_2S decomposition on metallic catalysts at room temperature. The sample was taken directly behind outlet of the catalytic reactor at the moment of equilibrium concentration of all products in the reaction mixture (Fig. 2)

Table 2 Hydrogen sulfide decomposition on the 0.5 % Pt/SiO_2 catalyst

No. exp.	Reaction temperature (°C)	H_2S supplied (mmol)	H_2S non-reacted (mmol)	H_2S conversion (%)	TON[a], mol H_2S/mol Pt
1	25	9.8	8.5	13.3	22
2	25	9.4	8.0	15.0	23
3	25	10	7.9	21.0	35
4	25	9.4	8.4	10.6	17 Total $\Sigma = 97$

Catalyst mass of 2 g was reduced in hydrogen at 400 °C. H_2S feeding is 2.5–3.0 ml/min, Ar feeding is 20 ml/min. Experiment duration is 60 min. Between experiments, no catalyst regeneration was undertaken

[a] Turn-over-number of the reaction calculated without considering Pt dispersion. For typical supported Pt catalysts prepared with impregnation, Pt dispersion is varied from 10 to 30 %, therefore to get a real TON, the values given should be multiplied by a factor from 3 to 10

conversion in the time-on-stream period at room temperature is (15 ± 5) %. The reaction turn-over-number is around 20 mol H_2S/mol Pt, that means the reaction is true catalytic one. Based on average conversion of H_2S in one experiment, a partial pressure of a substance with 64 m/z may be estimated as about 18 ± 5 torr.

A substantial regularity was observed for all metallic catalysts: as reaction temperature is increasing, conversion is decreasing and vice versa (Table 3). In a set of consecutive experiments, after catalyst testing at higher (lower) temperature, a control experiment was performed at room temperature. Table 3 shows a good reproducibility of catalyst activity. Unusual temperature dependence of H_2S decomposition is typical of bimolecular reactions occurring on the catalyst surface in an adsorbed layer, when at temperature increasing the surface coverage with adsorbed molecules is decreasing, which results in diminishing a probability of chemical interaction between two adjacent molecules.

By use of alumina as a carrier for supported metallic catalysts, division of reaction products of H_2S decomposition was fortunately accomplished (Fig. 5). On passing H_2S through the alumina supported metallic catalyst BIC-24-9, evolution of hydrogen is increasing with time, while gaseous sulfur evolution is very slight and comes down (Fig 5a). After ~3 h time-on-stream, the catalyst was isolated in a closed space, i.e. the reactor inlet and outlet were shut off. Overnight later, the reactor was blown through with argon, in gas phase only gaseous sulfur was detected, evolution of hydrogen was negligible (Fig. 5b). The total conversion of hydrogen sulfide in the adsorption–desorption cycle was 27.5 %, which is essentially higher in comparison with bulk and silica or Sibunit supported metallic catalysts. The experiment is well reproducible (Fig. 5), which means that alumina may serve as a reservoir to accumulate gaseous sulfur that can be removed by argon blowing through the catalyst. According to X-ray fluorescent analysis, surface concentration of sulfur adsorbed is ~0.5 % mass.

It is generally accepted that the electronic structure of diatomic sulfur is an analog of oxygen; therefore, the

Table 3 Temperature dependences of hydrogen sulfide decomposition on the Sibunit supported metallic catalyst BIC-24-10

No. exp.	Reaction temperature (°C)	Time-on-stream (min)	Amount of H_2S (mmol)		Conversion (%)	Productivity, ml H_2S converted/ml cat. h
			Supplied	Non-reacted		
7	25	40	3.8	3.3	13.3	8.4
8	100	40	3.7	3.5	5.7	3.5
9	25	40	3.7	3.3	12.4	7.7
12	200	45	4.2	4.1	2.8	1.8
13	25	40	3.8	3.3	13.3	8.4
14	250	40	3.8	3.7	1.3	0.8
15	25	40	3.8	3.3	12.5	7.9
16	0	40	3.8	3.1	17.9	11.25
18	25	40	4.0	3.5	12.3	8.2

Catalyst mass of 1.0 g was reduced in hydrogen at 400 °C. Feeding of Ar is 26 ml/min, H_2S—2.1 ml/min. No catalyst regeneration between experiments was undertaken

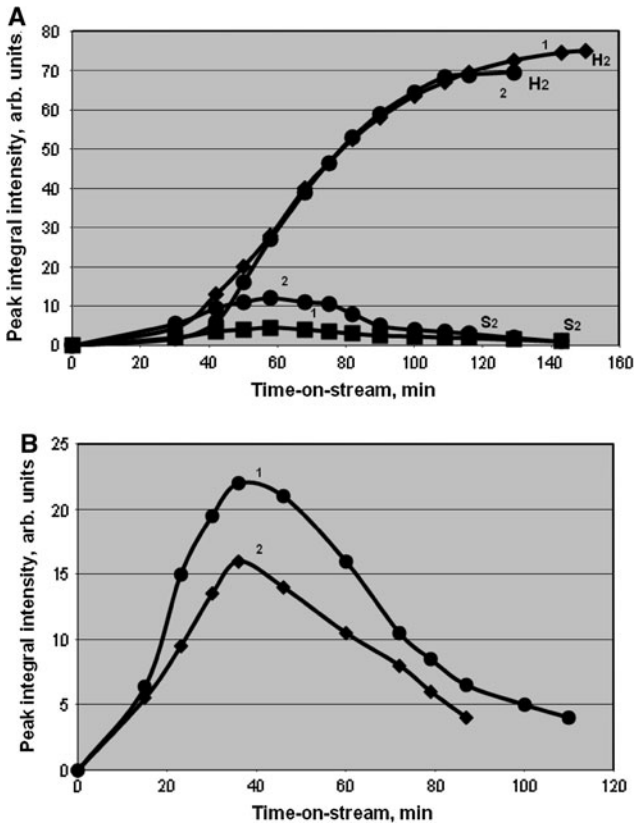

Fig. 5 **a**. Evolution of hydrogen and gaseous sulfur on passing H_2S at room temperature through the alumina supported metallic catalyst BIC-24-9. **b**. Desorption of gaseous sulfur from the catalyst surface later overnight after adsorption in Fig. 6a. No hydrogen evolution is detected. Two consecutive experiments are shown

molecule is in the ground triplet state $X\,^3\Sigma_g^-$ [27]. Calculation of electronic structure of S_2 molecule has shown that the ground state is really a triplet (Table 4). In DFT/B3LYP method the singlet with the closed shell is over for energy by 22.7 kcal/mol, but this state is unstable. Removal of the spin

Table 4 Calculated parameters of S_2 molecule in the electronic states of triplet, broken-symmetry singlet and excited singlet (in DFT—"cleaned singlet" being constituent of BS-singlet)

Parameter and method	Triplet	BS-singlet	Singlet
ΔE (kcal/mol)			
DFT/B3LYP	0.0	5.27	10.36
CASSCF(6e,6MO)	0.0	–	14.38
Bond length (Å)			
DFT/B3LYP	1.927	1.928	1.924
CASSCF(6e,6MO)	1.904	–	
Stretching mode (cm^{-1})			
DFT/B3LYP	684.0	683.4	688.4
CASSCF(6e,6MO)	735.2	–	

symmetry restriction resulted in the stable BS singlet with energy of 5.3 kcal/mol above the triplet state. The distinctive feature of the BS singlet obtained is the true diamagnetic state, but not a bi-radical as could be expected. This is caused by the structure of the upper occupied valence orbitals (Fig. 6). As follows from Fig. 6, the dimension and shape of orbitals for different spins are similar, but they are oriented in space in a different manner. As a result, the overlap integral of the corresponding α- and β- molecular orbitals is not equal to 1; this caused a spin contamination, however, their total contribution to the spin density on the atom is equal to 0. Detailed analysis of the wave function of BS singlet has shown that it is a mixture of the singlet and triplet states $\Psi_{BS} = a \cdot \Psi_S + b \cdot \Psi_T$ with almost equal weights ($a^2 = 0.498$, $b^2 = 0.502$). Because of this, singlet state cannot be represented with one-determinant function, therefore it cannot be found in a standard DFT calculation. The energy of this singlet state can be estimated as $E_S = (E_{BS} - b^2 \cdot E_T)/a^2$ and it is over the triplet ground state by 10.4 kcal/mol: (Scheme 1).

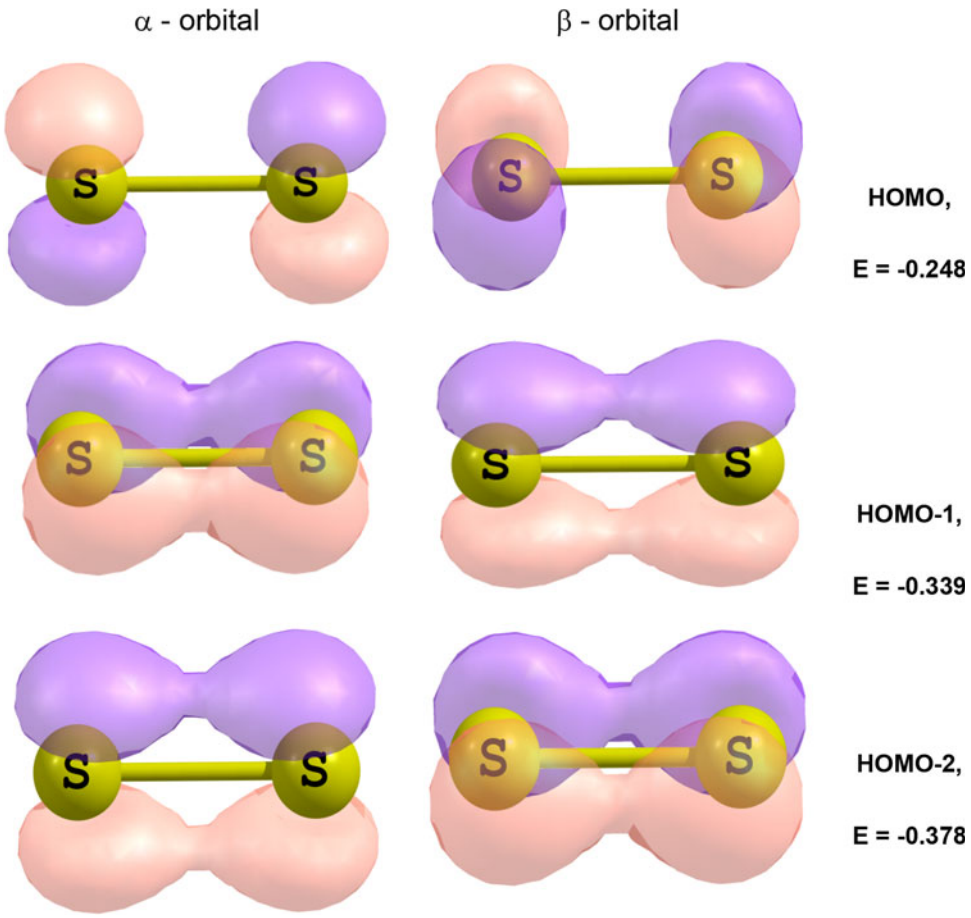

Fig. 6 View of the three upper occupied α- and β- molecular orbitals for BS singlet (*HOMO* high occupied molecular orbital). Orbital energy is in Hartree. Orbitals were drawn with a Chemcraft program [26]

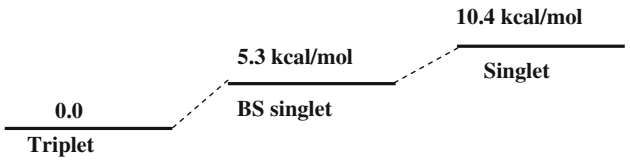

Scheme of energy level dispositions of the S_2 molecule

Scheme 1 Scheme of energy level dispositions of the S_2 molecule

One should note that bond length and stretching mode of both triplet and BS singlet differ insignificantly (Table 4). To estimate more accurately the energy and stability of the excited singlet state, we used CASSCF method. The calculated excitation energy from ground to singlet state is equal to 14.4 kcal/mol (Table 4).

The similar analysis made for atomic sulfur has shown that the ground stable state is a triplet, BS singlet is over in energy by 8.7 kcal/mol, while the singlet state is spaced from BS singlet by 17.5 kcal/mol. Unstable singlet state described with one-determinate function is over the triplet state by 38.6 kcal/mol. The calculations showed that the formation of the diatomic singlet sulfur from two singlet sulfur atoms results in the energy gain of 118.7 kcal/mol. Evidently, one may be presupposed that hydrogen sulfide decomposition can occur on the surface of metallic catalysts according to equation:

$$H_2S \Leftrightarrow H_2 + S_{ads} \quad (4)$$

caused by the formation of atomic singlet sulfur in the adsorbed state. Most probably, this mechanism is realized on the surface of alumina supported metallic catalysts BIC-24-9 (Fig. 5). In this case, after H_2S adsorption at room temperature predominantly only hydrogen evolves into gas phase (Fig. 5a), while the reaction limiting step is a surface reaction of the atomic singlet sulfur recombination into the singlet diatomic sulfur, which can be desorbed into gas phase by the catalyst flowing with argon overnight later after adsorption (Fig. 5b).

Starting from the triplet state of the diatomic sulfur, paramagnetic properties of this molecule should be expected by analogy with oxygen. In literature, we have found the only paper describing the EPR spectra at 8,880 MHz of diatomic sulfur obtained in situ by interaction of sulfur dichloride with hydrogen [28]. With that end in view, the EPR spectra[1] were recorded at room

[1] Authors are grateful to S.N. Truchan and O.N. Martyanov for EPR spectra recording.

temperature with a spectrometer EleXsys 500 in the region X ~ 9.5 GHz and Q ~ 34 GHz. In the first case, the sample of the BIC-24-9 catalyst with the gaseous sulfur adsorbed (Fig. 5a) was loaded into a quartz ampoule of ∅ 10 mm; the ampoule was evacuated at −100 °C and sealed. During EPR spectra recording of gaseous phase, the ampoule was heated to 100 °C, which presupposed sulfur desorption into gas phase. In the second case, the gas phase of product desorption (Fig. 5b) was passing through a quartz capillary of ∅ 1 mm and at the moment of maximum sulfur evolution, the capillary was isolated on both ends with paraffin. However, in both cases no EPR signal was detected. Therefore, one may evidently conclude that in the catalytic reaction of hydrogen sulfide decomposition on metallic catalysts at room temperate the diatomic gaseous sulfur in diamagnetic singlet state with the total spin equal to 0 is realized according to equation:

$$2H_2S \Leftrightarrow 2H_2 + S_2^{(gas)} \quad (5)$$

The arrangement of the formula (5) is in full agreement with the rule of spin conservation.

According to the equation, reaction (5) occurs with an increasing volume; therefore, to shift equilibrium to the right, one or both reaction products should be removed from the catalyst surface. The main idea to employ autoclave implies the use of a carrier to accumulate gaseous sulfur. Actually, alumina is found to be a very effective accumulator to keep gaseous sulfur in the adsorbed state (Table 5). H_2S conversion comes near 30 %, which is higher than the average conversion in gas flow regime. After autoclave was open to the atmosphere, it has been found that color of silica is dirty-grey and alumina is straw. After exposure to air in several days, both patterns had become colorless, while sulfur surface concentration did not change in this period.

In the UV spectra of diffuse reflection of sulfur adsorbed on alumina (sample 3 from Table 5), a strong absorbance is observed in the region above 30,000 cm^{-1} (Fig. 7), while a mechanical mixture of solid sulfur with alumina absorbs only slightly. In IR spectra of diffuse reflection of the former sample, a strong band at 809 cm^{-1} is observed (Fig. 8), which is absent in spectra of solid sulfur. This band can be attributed to the sulfur–sulfur stretching mode in the adsorbed state ν_{S-S}. The similar band at 830 cm^{-1} is found in the spectra of sulfur adsorbed on silica.

After 1.5 year storage of sample 3 from Table 5 in a closed vessel but under the air blanket, 25 g of this colorless sample was blown down with argon at room

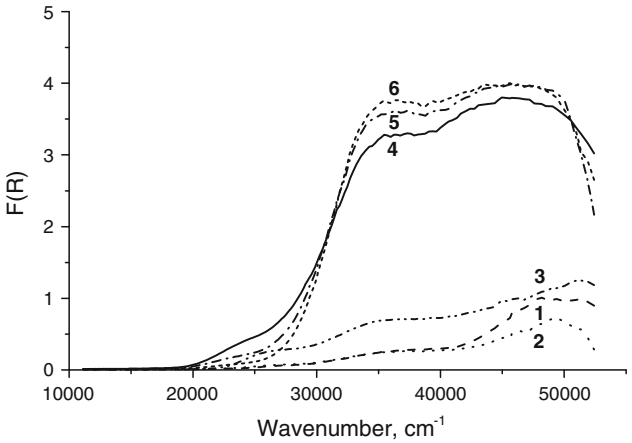

Fig. 7 UV spectra of diffuse reflection of gaseous sulfur adsorbed on alumina (sample 3, Table 5). Sulfur surface concentration is 2.07 %. *1* Initial alumina; *2*,*3* mechanical mixture of 1 and 10 % of solid sulfur with alumina; the mixture was prepared by careful grinding of the market sulfur and alumina in an agate mortar; *4* freshly prepared straw sample 3 from Table 5; *5* bright-yellow pattern after keeping sample 3 from Table 5 in a closed vessel for several hours; *6* colorless pattern after keeping sample 3 from Table 5 in air for several days

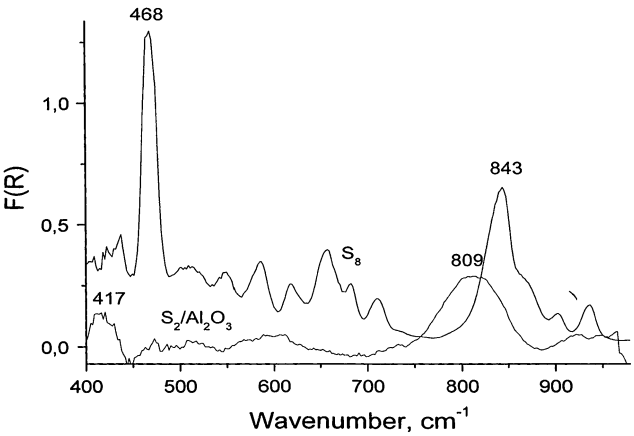

Fig. 8 Difference IR spectra of diffuse reflectance of gaseous sulfur adsorbed on alumina (sample 3 from Table 5) and solid market sulfur

Table 5 H_2S decomposition in autoclave at room temperature over the bulk catalyst BIC-24-7

Catalyst mass is 5 g. In autoclave, a freshly calcined carrier is loaded which is separated from the catalyst with a partition made of fiberglass

[a] X-ray fluorescent analysis

No.	Carrier	Carrier mass (g)	H_2S loading (g)	Sulfur content on carrier[a] (mass %)	Sulfur mass on carrier (g)	Yield of sulfur in reaction (5) (%)
1	Silica	47.0	2	0.14	0.07	3.3
2	Alumina	42.3	4	0.76	0.32	8.0
3	Alumina	54.6	4	2.07	1.13	28.2
4	Sibunit	50.1	5	0.82	0.41	8.2
5	Sibunit	66.7	5	0.39	0.26	5.2

temperature. During the blowing, gaseous sulfur was detected with a gas chromatograph. X-ray fluorescent analysis has shown that the sulfur surface concentration decreased from 1.006 % mass in the initial sample to 0.7021 % mass in the final sample, i.e., 0.076 g of sulfur was volatilized. The understated sulfur surface concentration in comparison with the freshly prepared sample 3 from Table 5 means that adsorbed sulfur still disappeared from the surface, however it does react with neither oxygen nor water of the air. Therefore, alumina can be used as an accumulator of gaseous sulfur, which might be easily claimed in case of need.

Another solution to shift equilibrium of the reaction (5) to the right consists in using solvents to dissolve sulfur formed. For this purpose, the reaction (5) was proposed to carry out in the trickle-bed regime after catalyst being immersed into liquid and H_2S being passed through the reactor [29–32]. In the case of aqueous monoethanolamine (MEA) solution, only hydrogen is detected in gas phase and H_2S conversion is close to 100 % (Table 6). In $\sim$2 h of time on stream, H_2S feeding is stopped and reactor is isolated in closed space. Overnight later, the reactor was blown down with argon, only hydrogen was detected in gas phase and H_2S was supplied again (Table 6). In four consecutive experiments the total H_2S conversion attained 99.6 % (Table 6). To recover sulfur from the solution, a very simple method can be used: after solution acidification with HCl until pH $\sim$2, yellow fine sulfur is precipitated. After separation on a paper filter, X-ray analysis has shown an orthorhombic modification of α-sulfur. However, the mother solution contains also sulfur; therefore, additional investigations should be undertaken to complete sulfur recovery from the solution. Nevertheless, the use of solvents seems to be the principal resolution of the problem of H_2S utilization at room temperature to obtain the target product—hydrogen [29–32].

Table 6 H_2S decomposition at room temperature over the bulk catalyst BIC-24-7 immersed into 5 % aqueous solution of monoethanolamine (MEA)

No. adsorption	Reaction duration (min)	H_2S (mmol)		H_2S conversion (%)
		Feeding	Non-reacted	
1	130	10.45	Traces	
2	111	8.91	Traces	
3	120	9.64	Traces	
4	270	21.7	Traces	
Σ		50.7	0.2	99.6

The Ar flow rate is 6 ml/min, H_2S is 1.8 ml/min, catalyst mass is 2 g, volume of solution is 150 ml

4 Discussion

Disulfane, H_2S_2, is the primary substance which gave impetus to research mechanism of its formation from H_2S on the surface of sulfide catalysts [15, 16] (reaction 2) despite its direct formation from H_2S in gas phase is thermodynamically prohibited (reaction 3). Disulfane is a yellow liquid with asphyxiating smell, a rather stable compound, but decomposes slowly in air to form sulfur and hydrogen sulfide [33]. However, thermodynamics of its decomposition does not exclude the possibility of hydrogen formation in accordance with equations:

$$H_2S_2 \leftrightarrow H_2 + S_2^{(gas)} \quad (6)$$

$\Delta_r H_{298}^\circ = 27.1$ kcal/mol, $\Delta_r S_{298}^\circ = 23.4$ cal/mol K, $\Delta_r G_{298}^\circ = 20.1$ kcal/mol, $\Delta_r G = 0$ at 1,158 K and

$$H_2S_2 \rightarrow H_2 + 1/4\, S_8^{(solid)} \quad (7)$$

$\Delta_r H_{298}^\circ = -3.8$ kcal/mol, $\Delta_r S_{298}^\circ = -29.2$ cal/mol K, $\Delta_r G_{298}^\circ = 4.9$ kcal/mol, $\Delta_r G = 0$ at 130 K (reference data for calculations are taken from [8]). In the first case, reaction (6) is endothermic and demands energy input from the outside. This mechanism can be evidently realized at high temperature [17]. The second mechanism (reaction 7) is typical most probably of sulfide catalysts [13, 14]. Thus, decomposition of hydrogen sulfide into constituent elements is thermodynamically favorable through the formation of the adsorbed disulfane as a key surface intermediate, but initiation of this process is impossible in gas phase without participation of catalyst surface.

Nevertheless, for metallic catalysts another possible pathway of H_2S decomposition seems to be realized. The molecular and dissociative adsorption of H_2S on the surface of transition metals is a highly exothermic process, which occurs at a low temperature (110 K) via very small energy barriers resulting in the formation of adsorbed atomic species [34, 35]. For small coverages, $\theta_S < 0.3$ ML, atomic sulfur is the most stable species' however, when the sulfur coverage increases on the surface, there is a substantial weakening in Pt–S interaction due to formation of S–S bond [36], and desorption of S_2 is now observed in thermo-desorption spectrum. The key to this behavior is probably a weakening of the metal–sulfur bonds that is compensated by S–S bonding. It is important that sulfur does not penetrate into sub-surface layer of Pt and does not form platinum sulfides.

Thus, H_2S decomposition at room temperature into constituent elements is thermodynamically favorable process via both adsorbed disulfane formation as a key surface intermediate and complete dissociation of H_2S to atoms at the metallic surfaces. However, the use of metallic catalysts has revealed unexpected and unpredictable experimental

outcome—the reaction product, along with hydrogen, is gaseous diatomic sulfur existing at normal conditions.

At present, extensive studies of sulfur properties in any aggregation state and at any external impacts are collected and classified [37–40]. Sulfur reactivity towards various substrates is considered, e.g. in [41, 42]. Thermodynamical properties of sulfur vapors are collected in [42–44].

Gaseous S_2 molecule obtained at thermal excitation of solid sulfur has the triplet ground state with the configuration $X\ ^3\Sigma_g^-$, equilibrium interatomic distance $r_e = 1.889$ Å, and the ground state vibration energy $\omega_e = 725.68\ cm^{-1}$ [27]. The molecule is paramagnetic at 1,000 K [45], the Raman shift at 718 cm^{-1} was assigned to the fundamental mode of S_2 vibration [46]. From UV absorption and fluorescence spectra of sulfur vapor the harmonic fundamental mode of the S_2 ground state was derived as $\omega_e = 726\ cm^{-1}$. The gas-phase EPR spectrum of diatomic sulfur was recorded in [28]. Diatomic molecule can be isolated only in the solid matrix of the inert gases on condensation of S_2 vapor [47–49], while on warming to room temperature it converts into "normal" solid orthorhombic sulfur. The ground state of S_2 molecule has been calculated using different methods [50–54].

Diatomic sulfur is isovalent with O_2 and has a similar electronic structure. Singlet oxygen chemistry is well developed [55, 56] and has initiated considerable interest in its analogous sulfur species, $^1S_2$. The physical properties of S_2 are well known, it exists in either singlet $^1S_2$ or triplet $^3S_2$ forms quite analogous to the two states of diatomic oxygen. A variety of methods for the generation of $^1S_2$ were discussed in [57–60], but none of them allowed isolating this substance in pure form. Singlet sulfur in situ synthesized was characterized by specific reactions with various substrates in analogy with singlet oxygen, in particular, with conjugated dienes [61] and anthracene [62]. Nevertheless, by means of this very reactive molecule, large amounts of new sulfur containing organic substances with unique properties were synthesized and characterized [63-66].

Diatomic gaseous sulfur obtained in the reaction (5) is characterized with loathsome sickening smell, is rather soluble in water up to 0.5 % mass, at temperature of liquid nitrogen is crystallized as white snowflakes, at room temperature reacts with Teflon (!) and silicone. The molecule is stable in adsorbed or dissolved states for a long period of time (weeks and months), does not react with water and oxygen at room temperature.

5 Conclusions

1. A new catalytic reaction of hydrogen sulfide decomposition is discovered, the reaction occurs on metal catalysts in flow gas phase according to equation

$$2H_2S \leftrightarrow 2H_2 + S_2^{(gas)}$$

to produce hydrogen and gaseous diatomic sulfur, conversion of hydrogen sulfide at room temperature is close to 15 %. When considering the temperature dependence of the reaction discovered, conversion of hydrogen sulfide decreases with rising temperature and at 250 °C the reaction is almost stopped.
2. The thermodynamic driving force of the reaction is the formation of the chemical sulfur–sulfur bond between two hydrogen sulfide molecules adsorbed on two adjacent metal atoms in the key surface intermediate and elimination of hydrogen into gas phase. Hereby, the solid catalyst ensures the possibility to realize surface reaction, which is thermodynamically prohibited in gas phase.
3. "Fingerprints" of diatomic sulfur adsorbed on the solid surfaces and dissolved in different solvents are studied. In closed vessels, this molecule is stable for a long period of time (weeks).
4. A possible electronic structure of diatomic gaseous sulfur in the singlet state is considered. According to DFT/CASSCF calculations, energy of the singlet state of S_2 molecule is over the ground triplet state energy for 10.4/14.4 kcal/mol. Some properties of gaseous diatomic sulfur are also investigated.
5. Catalytic solid systems, both bulk and supported on porous carriers, are developed. The supported catalysts are prepared by impregnation of a carrier with aqueous solution of cheap and nontoxic metal salts; the technology of catalyst preparation can be easily realized at any catalytic manufactures.
6. It was found that alumina is very effective accumulator to keep gaseous sulfur in the adsorbed state, which might be easily claimed in case of need by flowing with argon.
7. To shift equilibrium of hydrogen sulfide decomposition to formation of final products—hydrogen and sulfur, it is proposed to carry out the process on solid catalysts at room temperature under a layer of solvent capable of dissolving sulfur. In this case, a 100 % conversion of hydrogen sulfide can be achieved. This gives grounds to consider hydrogen sulfide as an inexhaustible potential source of hydrogen—environmentally clean energy source and valuable chemical product.

Acknowledgments A. N. S. and O. V. K. are grateful to Eni S.p.A. (Italy) for financial support in 2008.

References

1. Barreto L, Makihira A, Riahi K (2003) The hydrogen economy in the 21st century: a sustainable development scenario. Int J Hydrogen Energy 28(3):267–284

2. Midilli A, Ay M, Dincer I, Rosen MA (2005) On hydrogen and hydrogen energy strategies. I. current status and needs. Renew Sustain Energy Rev 9(3):255–271
3. Ohta T (2006) Some thoughts about the hydrogen civilization and the culture development. Int J Hydrogen Energy 31(2): 161–166
4. Goltsov VA, Veziroglu TN, Goltsova LF (2006) Hydrogen civilization of the future—a new conception of the IAHE. Int J Hydrogen Energy 31(2):153–159
5. James OO, Maity S, Mesubi MA, Ogunniran KO, Siyanbola TO, Sahu S, Chaubey R (2011) Towards reforming technologies for production of hydrogen exclusively from renewable resources. Green Chem 13:2272
6. Midili A, Ay M, Kale A, Veziroglu TN (2007) A parametric investigation of hydrogen energy potential based on H_2S in Black Sea deepwaters. Int J Hydrogen Energy 32:117–124
7. National Library of Medicine. Hydrogen sulfide (3/2/89). In: Hazardous substances data base (online file). Washington, D.C.: US DHHS, PHS, NIH, MEDLARS Management Section
8. Benson SW (1978) Termochemistry and kinetics of sulfur-containing molecules and radicals. Chem Rev 78(1):23–35
9. Kaloidas V, Papayannakos N (1987) Hydrogen production from the decomposition of hydrogen sulphide. Equilibrium studies on the system $H_2S/H_2/S_i$, $(i = 1,\ldots,8)$ in the gas phase. Int J Hydrogen Energy 12(6):403–409
10. Zaman J, Chakma A (1995) Production of hydrogen and sulfur from hydrogen sulfide. Fuel Process Technol 41:159–198
11. Luinstra EA (1995) Hydrogen from H_2S: technologies and economics. Sulfotech Research, May
12. Cox BG, Clarke PF, Pruden BB (1998) Economics of thermal dissociation of H_2S to produce hydrogen. Int J Hydrogen Energy 23(7):531–544
13. Startsev AN, Zakharov II, Voroshina OV, Pashigreva AV, Parmon VN (2004) Low-temperature decomposition of hydrogen sulfide under the conditions of conjugate chemisorption and catalysis. Dokl Phys Chem 399(1):283–286
14. Zakharov II, Startsev AN, Voroshina OV, Pashigreva AV, Chashkova NA, Parmon VN (2006) The molecular mechanism of low-temperature decomposition of hydrogen sulfide under conjugated chemisorption–catalysis conditions. Russ J Phys Chem 80(9):1403–1410
15. Aleshina GI, Aksenov DG, Startsev AN (1998) Use of thermoprogrammed technique to look for occluded hydrogen in the sulfide catalysts. Proceedings of international symposium on molecular aspects of catalysis by sulfides. Novosibirsk, p 100–102
16. Startsev AN, Aleshina GI, Aksenov DG (2001) Temperature-programmed heating to study sulfide catalysts: a comparison of reduction and desorption modes. Proceedings of 2nd international symposium on molecular aspects of catalysis by sulfides. Porqueroles, p 33
17. Raymont MED (1975) Make hydrogen from hydrogen sulfide. Hydrocarbon Process 7:139–142
18. Busev AI, Simonova LN (1975) Analytical chemistry of sulfur. Nauka, Moscow, p 66
19. Frisch MJ, Trucks GW, Schlegel HB (2009) Gaussian 09, Revision A.02. Gaussian Inc, Wallingford
20. Becke AD (1993) Density-functional thermochemistry. III. The role of exact exchange. J Chem Phys 98:5648–5652
21. Becke AD (1988) Phys Rev A 38:3098
22. Lee C, Yang W, Parr RG (1988) Phys Rev B 37:785
23. Vosko SH, Wilk L, Nusair M (1980) Can J Phys 58:1200
24. McLean AD, Chandler GS (1980) J Chem Phys 72:5639–5648
25. Krishnan R, Seger JS, Pople JA (1980) J Chem Phys 72:650–661
26. Zhurko GA Program Chemcraft. www.chemcraftprog.com. Accessed 6 May 2012
27. Huber KP, Herzberg G (1979) Molecular spectra and molecular structure. IV. Constants of diatomic molecules. Van Nostrand Reinhold Co., New York, p 564
28. Wayne FD, Davies PB, Thrush BA (1974) The gas-phase E.P.R. spectrum of diatomic sulphur molecules. Mol Phys 28(4): 989–996
29. Startsev AN, Pashigreva AV, Voroshina OV, Zakharov II, Parmon VN (2005) RF Patent 2,261,838, 10 Oct 2005
30. Startsev AN, Pashigreva AV, Voroshina OV, Zakharov II, Parmon VN (2007) Ukraine Patent 81,088, 26 Nov 2007
31. Startsev AN, Pashigreva AV, Voroshina OV, Zakharov II, Parmon VN (2008) Kazakhstan Patent 57,481, 15 Dec 2008
32. Startsev AN, Pashigreva AV, Voroshina OV, Zakharov II, Parmon VN, (2007) US Patent 7,611,685, 3 Nov 2009
33. Feher F, Laue W, Winkhaus G (1956) Uber die Darstellung der Sulfane H_2S_2, H_2S_3, H_2S_4 und H_2S_5. Z anorg Algem Chemie 288(3–4):113
34. Alfonso DR (2008) First-principles studies of H_2S adsorption and dissociation on metal surfaces. Surf Sci 602:2758–2768
35. Koestner RJ, Salmeron M, Kollin EB, Gland JL (1986) Adsorption and surface reactions of H_2S on clean and S-covered Pt(111). Surf Sci 172(3):668–690
36. Rodriguez JA, Hrbek J, Kuhn M, Jirsak T, Chaturvedi S, Maiti A (2000) Interaction of sulfur with Pt(111) and Sn/Pt(111): effects of coverage and metal–metal bonding on reactivity toward sulfur. J Chem Phys 113(24):11284–11292
37. Meyer B (1965) Elemental sulfur: chemistry and physics. Interscience, New York
38. Schmidt M (1962) Sulfur polymers. In: Stone FGA, Graham WGA (eds) Inorganic polymers. Academic Press, New York, p 98
39. Muller A, Krebs B (eds) (1984) Sulfur—its significance for chemistry, for geo-, bio-, and cosmosphere and technology. Elsevier, Amsterdam
40. Steudel IR (ed) (2003) Elemental sulfur and sulfur-rich compounds. Springer, Heidelberg
41. Pryor W (1962) Mechanisms of sulfur reactions. McGraw-Hill Book Co., Inc, New York
42. Chao J (1980) Properties of elemental sulfur. Hydrocarbon Process 10:217
43. Rau H, Kutty TRN, de Carvalho JRFG (1973) Thermodynamics of sulfur vapor. J Chem Thermodyn 5:833–844
44. Steudel R, Steudel Y, Wong MW (2003) Speciation and thermodynamics of sulfur vapor. Top Curr Chem 230:117–134
45. Meschi DJ, Searcy AW (1969) Investigation of the magnetic moments of S_2, Se_2, Te_2, and Se_5 by the Stern–Gerlach magnetic deflection method. J Chem Phys 51(11):5134–5138
46. Yee KK, Barrow RF, Rogstad A (1972) Resonance fluorescence and Raman spectra of gaseous sulfur. JCS Faraday II 68:1808–1811
47. Brewer L, Bradson GD, Meyer B (1965) UV absorption spectrum of trapped S_2. J Chem Phys 4(4):1385–1389
48. Brewer L, Bradson GD (1966) Ultraviolet fluorescent and absorption spectra of S_2 isolated in inert-gas matrices. J Chem Phys 44(9):3274–3278
49. Barletta RF, Claassen HH, McBeth RL (1971) Raman Spectrum of S_2. J Chem Phys 55(11):540910
50. Swope WC, Lee Y-P, Schafer HF (1979) Diatomic sulfur: low lying bound molecular electronic state of S_2. J Chem Phys 70(2):947–949
51. Hohl D, Jones RO, Car R, Parrinello M (1988) Structure of sulfur clusters using simulated annealing: S_2 to S_{13}. J Chem Phys 89(11):6823–6835
52. Suontamo RJ, Laitinen RS, Pakkanen TA (1994) Molecular valence calculations on small clusters S_2 to S_5. J Mol Struct (Theochem) 313:189–197

53. Millerfiori S, Alparone A (2001) Ab initio study of the structure and polarizability of sulfur clusters, S_n (n = 2–12). J Phys Chem A 105:9489
54. Jones RO, Ballone P (2003) Structure and bonding in S_n ring and chains (n = 2–18). J Chem Phys 118(20):9257
55. Kearns DR (1971) Physical and chemical properties of singlet molecular oxygen. Chem Rev 71(4):395–427
56. Schweitzer C, Schmidt R (2003) Physical mechanisms of generation and deactivation of singlet oxygen. Chem Rev 103(5):1685–1757
57. Steliou K (1991) Diatomic sulfur. Acc Chem Res 24(11):341–350
58. Harpp DN (1997) The sulfur diatomic: generation and trapping chemistry. Phosphorus Sulfur Silicon 120 & 121: 41–59
59. Abu-Yousef IA (2006) The oraganic chemistry of diatomic sulfur. J Sulfur Chem 27(1):87–119
60. Zysman-Colman E, Harpp DN (2007) Fascinating organosulfur functionalities: polyhalcogens as diatomic sulfur sources. Heteroat Chem 18(5):449–459
61. Steliou K, Gareau Y, Harpp DN (1984) "S_2": generation and synthetic application. J Am Chem Soc 106(3):799–801
62. Ando W, Sonobe H, Akasaka T (1987) Generation of singlet diatomic sulfur from 9,10-epidithio-9,10-dihidroanthracene. Tetrahedron Lett 28(52):6653–6656